Characteristics of electron temperature profile stiffness in electron-heated plasmas on EAST

J.W.Liu[1,2,3], Y.F.Liang[1,3,*], Q.Zang[1,*], Y.H.Huang[1], E.Z.Li[1], L.Q.Xu[1], Y.Q.Chu[1], Y.F.Jin[1,2], H.Q. Liu[1], H.L.Zhao[1], X.Z. Gong[1] and EAST team[1]

[1] *Institute of Plasma Physics, Chinese Academy of Sciences, PO Box 1126, Hefei 230031, People's Republic of China*

[2] *University of Science and Technology of China, Hefei 230026, People's Republic of China*

[3] *Forschungszentrum Jülich GmbH, Institut für Energie- und Klimaforschung – Plasmaphysik, Partner of the Trilateral Euregio Cluster (TEC), 52425 Jülich, Germany*

Abstract

Power balance analysis shows that the increase of ECRH power can increase the normalized T_e gradient significantly at the plasma core region ($\rho < 0.6$), but does not change the T_e profile stiffness in the low-density L-mode plasmas. Furthermore, three distinguishable stages characterized by different T_e profile stiffnesses can be identified from the density ramp-up in the electron heating dominant plasma on EAST. A formation of internal plasma density transport barrier at $\rho = 0.6$, accompanied by a sudden drop in core T_e and a rise in both of core density and ion temperature, has been observed for the first time when $<n_e>$ reaches a threshold of $2.2 \times 10^{19} m^{-3}$.

Introduction

It is foreseen that the high energy alpha particles created in the deuterium-tritium (DT) fusion reaction will give priority to heating electrons and then heat ions through electron-ion collisions [1]. Therefore, the study of electron temperature profile and heat transport properties for electron heating dominant plasmas is an important research topic and has been extensively carried out in many tokamak and stellarator devices. The experimental results demonstrated a threshold in the normalized electron temperature gradient R/L_{Te} , and above which the turbulence transport increases with R/L_{Te}. Normalized electron temperature gradient R/L_{Te} and electron heat flux q_e^{GB} (in gyro-Bohm units) can be used to characterize electron temperature profile stiffness S* [2] ($S^* = \frac{\partial q^{GB}}{\partial R/L_{\mathrm{T}}}$, $q^{GB} = \frac{qeBR^2}{nT^2\rho_s}$, $\rho_s = \frac{(m_i T)^{1/2}}{eB}$). where R is the plasma major radius, T is the electron temperature, n is the electron density, B is the toroidal magnetic field.

Experimental Advanced Superconducting Tokamak (EAST) [3,4] is an electron heating dominated tokamak device, which designed to achieve the long-pulse steady-state high-performance H-mode plasmas at ITER-like configurations and RF wave heating schemes.

Recently, EAST has been upgraded with installation of two new ECRH systems, and can be able to establish a stable long-pulse operation scenario with very high core electron temperature (T_{e0}~$10keV$). This provides a good platform for characteristics of T_e profile stiffness and plasma transport in electron heating dominant plasmas.

Experimental results

On EAST, a very high central electron temperature of about 10 keV has been achieved and stably maintained in electron heating dominated plasmas by applying a 4.6 GHz LHW with two on-axis power deposited ECRHs simultaneously. Figure 1 shows an overview of main plasma parameters from this experiment. Compared with the single ECRH heating stage, the central electron temperature increases significantly after the second ECRH injection at t=3.1s. As well as the normalized electron temperature gradient increased about 50% at ρ~0.2-0.4.

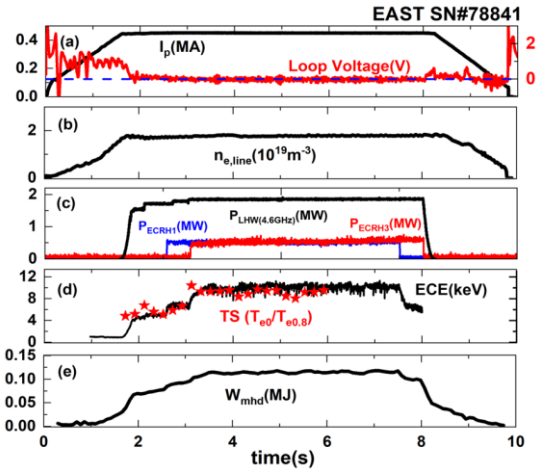

Figure 1. Main plasma parameters of EAST SN#78841.

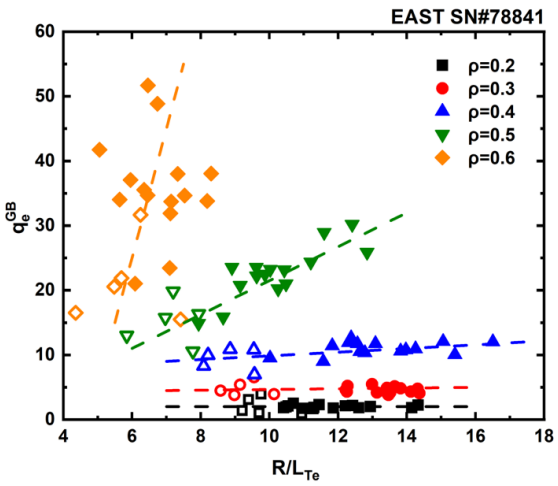

Figure 2. Variation of q_e^{GB} with R/L_{Te}

Figure 2 shows the variation of electron heat flux q_e^{GB} (in gyro-Bohm units) with the normalized electron temperature gradient R/L_{Te}. The dashed guide line shows the ratio between electron heat flux q_e^{GB} and normalized electron temperature gradient R/L_{Te}, which yield the slope to represent the T_e profile stiffness (S*). The result shows that the increase of ECRH power can increase the normalized T_e gradient significantly at the plasma core region ($\rho < 0.4$), but does not change the T_e profile stiffness. For quantitatively, the electron heat flux q_e^{GB} does not increase dramatically with the normalized electron temperature gradient R/L_{Te} inside $\rho < 0.4$. It indicates that the T_e profile stiffness is extremely weak or has been broken inside $\rho < 0.4$. From the growth rate and frequency of most unstable modes calculated by TGLF, the main instability modes are the medium wavelength low-k ($k_y < 1$) TEM.

Furthermore, a slow density ramp-up has been performed in the high core T_e L-mode plasma on EAST. In this experiment, the target plasma was sustained by 1.6MW LHW at 4.6GHz and three on-axis ECRH injections with a total power of 1.25 MW. The time evolutions of major plasma parameters of this discharge are shown in figure 3. During the plasma current plateau ($I_p = 0.55$MA) over 6 seconds, the central line averaged electron density has a slow ramp-up from $1.5 \times 10^{19} m^{-3}$ to $3.3 \times 10^{19} m^{-3}$. Three distinguishable stages characterized by different $T_e$profile stiffness can be identified from the density ramp-up, and they can be divided into the first stage (Stage-I: 2.5s-3.5s), the second stage (Stage-II: 3.5s-6s) and the third stage (Stage-III: 6s–9s), respectively. The trend of three stages also can be seen from the kinetic profiles (as shown in figure 4).

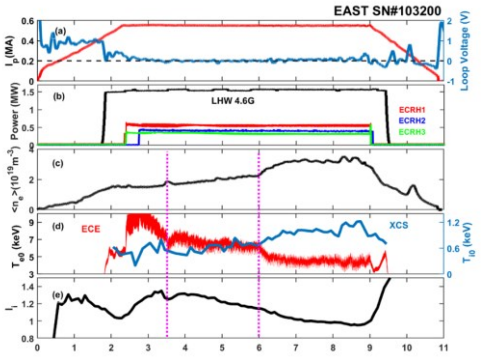

Figure 3. Main plasma parameters of EAST SN#103200.

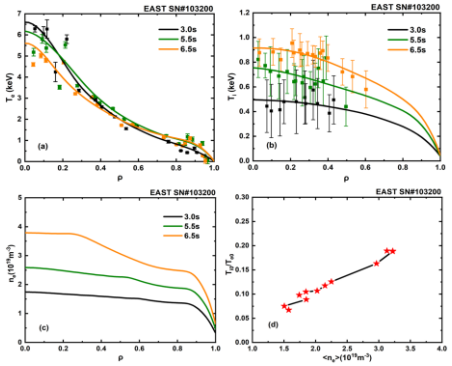

Figure 4. Kinetic profiles of EAST SN#78841.

Significantly different in the radial profiles of the normalized electron temperature gradient R/L_{Te}, and the normalized electron density gradient R/L_{ne}, are also observed in the above three stages (figure 5). Due to the normalized electron temperature gradient (R/L_{Te}) decreases rapidly following the electron heat flux (q_e^{GB}) reduces, the T_e profile stiffness at $\rho = 0.3$ is relatively weak in the first stage (figure 6). And the drop of the low-k ($k_y < 1$) TEM modes is consistent with the decrease of the core T_e gradient (R/L_{Te}). Next, a strong T_e profile stiffness

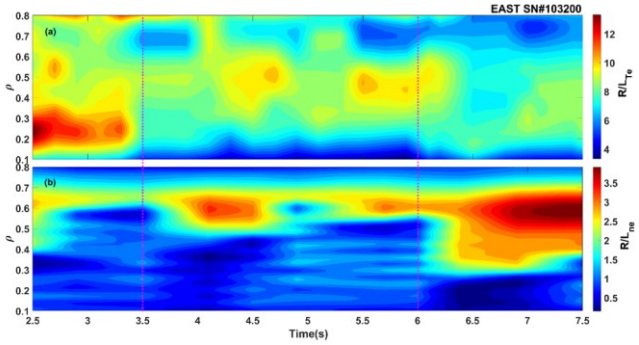

Figure 5. Time evolution of R/L_{Te} and R/L_{ne}.

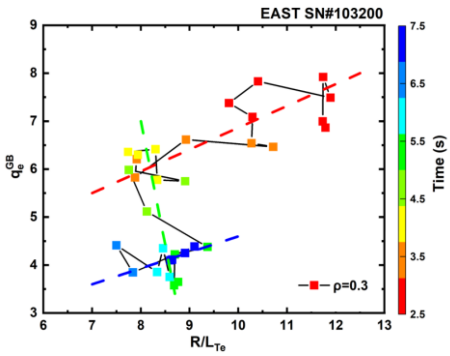

Figure 6. T_e profile stiffness.

at $\rho = 0.3$ can be observed in the second stage, where the core T_e gradient does not change significantly with the n_e increases. Current analysis shows that the LHW power deposition moves away from the plasma core region following the n_e increases. However, in the third stage, the T_e profile stiffness becomes much weaker than the other stages. Furthermore, a density internal transport barrier (as show in the figure 7(b)) appears at $\rho = 0.6$ after 6s, accompanied by a sudden drop in core T_e and a rise in both of core n_e and T_i (the core T_i increased by 20%), has been observed for the first time during the transition from the second stage to the third stage when the central line-averaged plasma density reaches a threshold of $2.2 \times 10^{19} m^{-3}$. It also turns out that the density internal transport barrier at $\rho = 0.6$ can be stably sustained even with a higher plasma density of $3.3 \times 10^{19} m^{-3}$. The study on T_e profile stiffness would support for the exploration of breaking stiffness in electron heating dominant plasmas on EAST and future ITER.

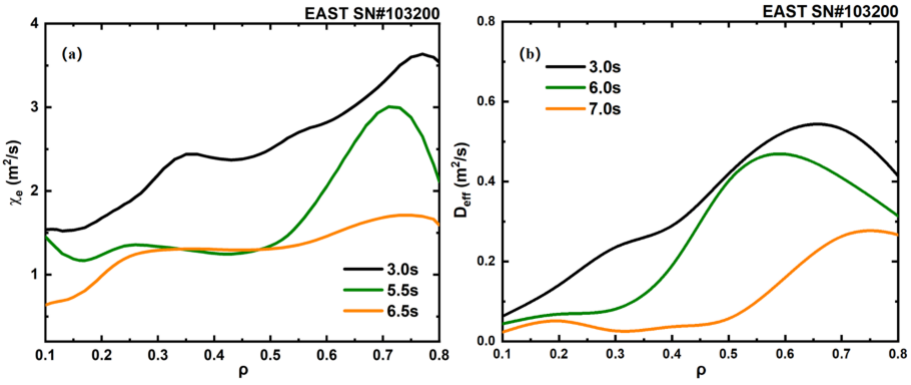

Figure 7. Transport coefficients of (a) effective electron thermal diffusivity, and (b) diffusivity calculated by power balance analyses.

Acknowledgements

This work is supported by the National Key R&D Programs of China under Grant No.2017YFE0301105, and Users with Excellence Program of Hefei Science Center, CAS，Contract No. 2021HSC-UE012, the National Natural Science Foundation of China under Contract No. 11905144. The numerical calculations in this paper were performed on the ShenMa High Performance Computing Cluster in Institute of Plasma Physics, Chinese Academy of Sciences.

References

[1] F. Ryter et al 2006 Plasma Phys. Control. Fusion 48 B453-B463.

[2] P. Mantica et al 2009 Phys. Rev. Lett. 102, 175002.

[3] J. Li et al 2011 Nucl. Fusion 51 094007.

[4] B.N. Wan et al 2017 Nucl. Fusion 57 102019.